Sensorless Control of Induction Motor Drives at Very Low and Zero Speeds Using Neural Network Flux Observers

Shady M. Gadoue, *Member, IEEE*, Damian Giaouris, *Member, IEEE*, and John W. Finch, *Senior Member, IEEE*

***Abstract*—A new method is described which considerably improves the performance of rotor flux model reference adaptive system (MRAS)-based sensorless drives in the critical low and zero speed regions of operation. It is applied to a vector-controlled induction motor drive and is experimentally verified. The new technique uses an artificial neural network (NN) as a rotor flux observer to replace the conventional voltage model. This makes the reference model free of pure integration and less sensitive to stator resistance variations. This is a radically different way of applying NNs to MRAS schemes. The data for training the NN are obtained from experimental measurements based on the current model avoiding voltage and flux sensors. This has the advantage of considering all drive nonlinearities. Both open- and closed-loop sensorless operations for the new scheme are investigated and compared with the conventional MRAS speed observer. The experimental results show great improvement in the speed estimation performance for open- and closed-loop operations, including zero speed.**

***Index Terms*—Flux estimation, induction motor, model reference adaptive system (MRAS), neural networks (NNs), sensorless control.**

I. Introduction

THERE HAS been much recent development of sensorless vector-controlled induction motor drives for high-performance industrial application [1]. Such control reduces the drive cost, size, and maintenance requirements while increasing the system reliability and robustness. However, parameter sensitivity, high computational effort, and stability at low and zero speeds can be the main shortcomings of sensorless control. Much recent research effort is focused on extending the operating region of sensorless drives near zero stator frequency [2], [3].

Several solutions for sensorless control of induction motor drives have been proposed based on the machine fundamental excitation model and high frequency signal injection methods, as summarized recently [1]. Fundamental model-based strategies use the instantaneous values of stator voltages and currents to estimate the flux linkage and motor speed. Various techniques have been suggested, such as model reference adaptive system (MRAS), Luenberger and Kalman-filter observers, sliding-mode observers, and artificial intelligence techniques. MRAS schemes offer simpler implementation and require less computational effort compared to other methods and are therefore the most popular strategies used for sensorless control [3], [4].

Various MRAS observers have been introduced in the literature based on rotor flux, back electromotive force, and reactive power [5]–[8]. However, rotor flux MRAS, first introduced by Schauder [6], is the most popular MRAS strategy, and significant attempts have been made to improve its performance [1]. This scheme suffers from parameter sensitivity and pure integration problems [7] which may limit the performance at low and zero speed regions of operation [5].

Online adaptation of the stator resistance can improve the performance of the MRAS sensorless drive at low speed [9]. In [4], a simultaneous estimation of rotor speed and stator resistance is presented based on a parallel MRAS observer, where both the reference and adaptive models switch roles based on two adaptive mechanisms. Moreover, pure integration for flux represents a crucial difficulty which may cause dc drift and initial condition problems [2], [7], [10]. Low-pass filters (LPFs) with low cutoff frequency have been proposed to replace the pure integrator [11]. This introduces phase and gain errors and delays the estimated speed relative to the actual, which may affect the dynamic performance of the drive [12], [13] in addition to inaccurate speed estimation below the cutoff frequency [7]. To overcome this problem, Karanayil *et al.* [12] introduce a programmable cascaded LPF to replace the pure integration by small time constant cascaded filters to attenuate the dc offset decay time. In [14], another technique is used, where the rotor flux is estimated by defining a modified integrator having the same frequency response as the pure integrator at steady state. A nonlinear feedback integrator for drift and dc offset compensation has been proposed in [15]. Further research has tried to entirely replace the voltage model (VM) with a state observer with current error feedback or full order stator and rotor flux observers, which reduces the scheme's simplicity [10], [16].

Neural networks (NNs) have been introduced as universal function approximators to represent functions with weighted sums of nonlinear terms [17]. Multilayer feedforward NNs have shown a great capability to model complex nonlinear dynamic systems [18]. Various attempts to model machine flux

Manuscript received January 17, 2008; revised May 21, 2009. First published June 10, 2009; current version published July 24, 2009.

S. M. Gadoue is with the Department of Electrical Engineering, Faculty of Engineering, Alexandria University, Alexandria 21544, Egypt (e-mail: Shady.Gadoue@ncl.ac.uk).

D. Giaouris and J. W. Finch are with the School of Electrical, Electronic and Computer Engineering, Newcastle University, Newcastle upon Tyne, NE1 7RU U.K. (e-mail: Damian.Giaouris@ncl.ac.uk; J.W.Finch@ncl.ac.uk).

Digital Object Identifier 10.1109/TIE.2009.2024665

from measured quantities, such as stator voltages, currents, and motor speed, have been discussed [17]–[20]. A comprehensive review of applications of NNs in the field of power electronics and motor drives is covered in [21].

NNs have been used before with MRAS schemes. In [22], an artificial NN (ANN) detects the thermal variations in the stator resistance at different operating conditions. Better low speed operation was shown when this ANN open-loop model is combined with the MRAS observer. NNs were also combined with MRAS for online stator and rotor resistance estimation based on stator current and rotor flux [23]. In [11], a two-layer linear NN is proposed to represent the conventional adaptive current model (CM) using a simple forward Euler integration method. The estimated speed represents one of the NN weights updated online using a back propagation algorithm. An evolution to this scheme is presented in [24] and [25], where an adaptive linear NN is employed in the adaptive model using the modified Euler integration to represent the CM. The ordinary least square algorithm is used to train the NN online to obtain the rotor speed information. An NN has also been presented as an adaptive filter used for signal integration to eliminate the offset in the flux integration for the VM flux observer [25], [26].

This paper describes a completely novel application of the NN for MRAS. This new MRAS scheme employs an NN rotor flux observer to entirely replace the conventional VM (and not the CM, as described in [11] and [24]) to improve the sensorless drive performance at low and zero speeds. A multilayer feedforward NN estimates the rotor flux from present and past samples of the terminal voltages and currents. Compared to a VM flux observer, NN does not employ pure integration and is less sensitive to motor parameter variations. Compared to other conventional schemes that make use of an LPF for flux estimation, the NN observer does not employ any filtering. This avoids delaying the estimated speed and prevents estimation errors below the filter cutoff frequency. The training data for the NN are obtained from experimental measurements, giving a more accurate model that includes all drive nonlinearities. This avoids using search coils which are not a suitable way to obtain flux measurements in most applications [17]. In this paper, outputs from the CM are used as target values for the NN to provide harmonic-free signals and an accurate output at low speed. An experimental implementation of the new NN-MRAS observer is described. The training was done at 0%–25% load, reflecting the expected application, but additional tests at 100% load are also included. The new NN scheme is compared with the conventional scheme, which employs a VM for flux estimation, in both open- and closed-loop sensorless modes for an indirect vector control induction motor drive. The drive performance is tested when running at very low and zero speeds at various load levels. Experimental results confirm the great improvement in the performance of the MRAS observer.

II. Rotor Flux MRAS Speed Observer

The classical rotor flux MRAS speed observer structure shown in Fig. 1 consists of a reference model, an adaptive model, and an adaptation scheme which generates the estimated speed. The reference model, usually expressed as a VM, represents the stator equation. It generates the reference value of the rotor flux components in the stationary reference frame from the stator voltage (estimated to avoid a direct measurement, as discussed later) and monitored current components. The reference rotor flux components obtained from the reference model are given by [6], [7]

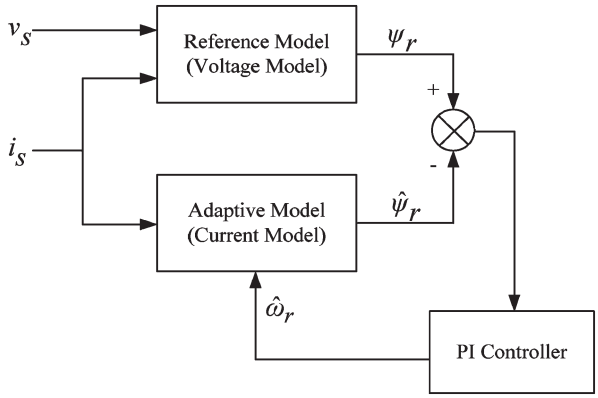

Fig. 1. Classical rotor flux MRAS speed observer.

$$p\psi_{rd} = \frac{L_r}{L_m}\{\nu_{sD} - R_s i_{sD} - \sigma L_s p i_{sD}\} \tag{1}$$

$$p\psi_{rq} = \frac{L_r}{L_m}\{\nu_{sQ} - R_s i_{sQ} - \sigma L_s p i_{sQ}\}. \tag{2}$$

The adaptive model, usually represented by the CM, describes the rotor equation, where the rotor flux components are expressed in terms of stator current components and rotor speed. The rotor flux components obtained from the adaptive model are given by [6], [7]

$$p\hat{\psi}_{rd} = \frac{L_m}{T_r} i_{sD} - \frac{1}{T_r}\hat{\psi}_{rd} - \hat{\omega}_r \hat{\psi}_{rq} \tag{3}$$

$$p\hat{\psi}_{rq} = \frac{L_m}{T_r} i_{sQ} - \frac{1}{T_r}\hat{\psi}_{rq} + \hat{\omega}_r \hat{\psi}_{rd}. \tag{4}$$

Based on Popov's hyperstability theory, the adaptation mechanism can be designed to generate the value of the estimated speed used so as to minimize the error between the reference and estimated fluxes [7], [8]. In the classical rotor flux MRAS scheme, this is done by defining a speed tuning signal ε_ω minimized by a proportional–integral (PI) controller which generates the estimated speed that is fed back to the adaptive model. The expressions for the speed tuning signal and the estimated speed can be given as [7]

$$\varepsilon_\omega = \psi_{rq}\hat{\psi}_{rd} - \psi_{rd}\hat{\psi}_{rq} \tag{5}$$

$$\hat{\omega}_r = \left(k_p + \frac{k_i}{p}\right)\varepsilon_\omega. \tag{6}$$

The main problems associated with the low speed operation of model-based sensorless drives are related to machine parameter sensitivity, stator voltage and current acquisition, inverter nonlinearity, and pure integration for flux. Since all model-based estimation techniques rely on rotor-induced voltage, which is very small and even vanishes at zero stator frequency, these techniques fail at or around zero speed [2].

A. Parameter Sensitivity

Since the speed estimation is based on the machine model, it is highly sensitive to machine parameter variations. Stator resistance variation with machine temperature is the most serious problem at low speed. Since the fundamental component of the stator voltage becomes very low, the stator resistance drop becomes comparable to the applied voltage. Hence, continuous adaptation of the stator resistance is required to maintain stable operation at low speed.

B. Stator Voltage Acquisition and Inverter Nonlinearity

The most accurate stator voltage acquisition is that measured across the machine terminals. This cannot be used easily since it requires a very high sampling rate [2]. Low-pass filtering the PWM voltage waveform may solve the problem at medium and high speeds but not at low speed, where the effect of filter gain and phase error causes performance to deteriorate. A synchronous integrator technique can aid a solution. However, not using voltage sensors is preferred in industrial applications. Using the reference voltages, available in the control unit, is possible since they are harmonic free. However, at low speed, these reference voltages deviate substantially from the actual machine voltages due to inverter dead time effects and inverter nonlinearities due to the characteristics of the power switches, including threshold voltages and voltage drops.

C. Stator Current Acquisition and Pure Integration Problems

Errors in the measured currents can be due to unbalanced gains of the measurement channels, dc offset, and drift. This may cause oscillation in the measured speed [27].

Rotor flux estimation based on VM needs open-loop integration for flux calculation. This pure integration is difficult to implement because of dc drift and initial condition problems. Replacement of pure integration by an LPF may help [7], [14], [26]. However, the flux estimation deteriorates below the filter cutoff frequency.

III. NN-MRAS Observer

To overcome these problems of the conventional RF-MRAS scheme, an NN was used to completely replace the VM. The training of this network was based on the CM, and hence, the MRAS scheme effectively uses two versions of the CM—one based on (3) and (4) and the other based on the trained NN. This greatly improves the performance of the speed estimator, as will be experimentally proved later. This section briefly describes various network topologies and training methods; a 0%–25% load range was used. A range reflecting the application is required for best performance, e.g., 0%–100% if high loads at very low speeds are expected.

The unit of structure of ANN is the neuron, which consists of a summer and an activation function. The most common type of ANN is the multilayer feedforward NN which consists of layers; each layer consists of neurons [11], [17].

Consider a neuron j in a layer m with n inputs in the $(m-1)$ layer and a threshold (b). The net input to the neuron is given by

$$net_j = \sum_{k=1}^{n} w_{jk}x_k + b_j = w_{j1}x_1 + w_{j2}x_2 + \cdots + w_{jn}x_n + b_j. \tag{7}$$

Moreover, the neuron output is given by

$$y_j = g(net_j) = g\left(\sum_{k=1}^{n} w_{jk}x_k + b_j\right) \tag{8}$$

where (g) is the activation function or the neuron transfer function.

Here, an 8-25-2 multilayer feedforward NN is used to estimate the rotor flux components in the stationary reference frame. To obtain good estimation accuracy, the inputs to the network are the present and past values of the d–q components of the stator voltage and current in the stationary reference frame. Compensated versions of the reference voltages are used, as discussed later. One of the major drawbacks of NN is the lack of design techniques. Hence, the number of neurons in the hidden layer is chosen by a trial-and-error technique to compromise between computational complexity, if a larger number is selected, and approximation accuracy, if a smaller number is selected [18]. This degree of trial and error may increase the training process time. The output layer consists of two neurons representing the rotor flux components in the stationary reference frame. Since the case is approximating a nonlinear function with bipolar input/output pattern, hyperbolic tan (*tansigmoid*) activation functions will be used in both hidden and output layers [21]. In this case, the neuron transfer function can be written as

$$y_j = \tanh(net_j) = \frac{1-\exp(-net_j)}{1+\exp(-net_j)}. \tag{9}$$

In this type of learning, a set of input/target data is used to train the NN [21]. At each sample, the NN output is compared with the target value, and a weight correction via a learning algorithm is performed to minimize the error between the two values [18], [22].

Once trained, the NN gives a fast execution speed due to its parallel processing [18], [21]. The offline-trained NN is used as a reference model for the MRAS observer to form the new NN-MRAS scheme, as shown in Fig. 2.

IV. Experimental System

The experimental platform that consists of a 7.5-kW 415-V delta-connected three-phase induction machine loaded by a 9-kW 240-V 37.5-A separately excited dc load machine allows separate control of load torque and speed. A 15-kW four quadrant dc drive from the Control Techniques "Mentor" range is used to control the dc machine to provide different levels of loading on the induction machine up to full load. The parameters of the induction machine are shown in the Appendix.

The ac drive power electronics consists of a 50-A three-phase diode bridge and 1200-V 50-A half-bridge insulated-gate

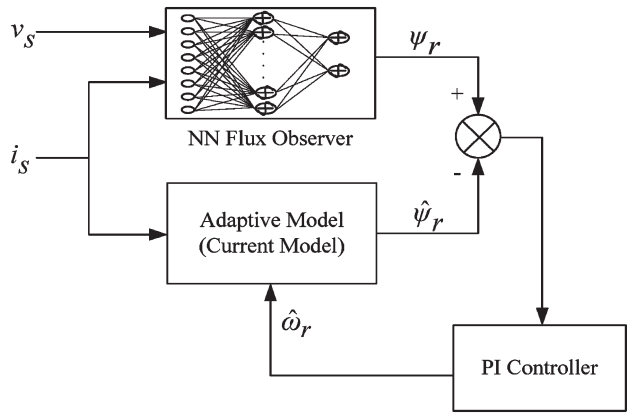

Fig. 2. Proposed NN-MRAS speed observer.

bipolar transistor power modules. To control the induction motor, a dSPACE system is used, which contains a PowerPC 604e running at 400 MHz and a Slave TMS320F240 DSP.

Hall effect current sensors were used to measure the motor line currents. The actual motor speed is measured by a 5000 pulses/revolution speed encoder. The inverter switching frequency is 15 kHz, and the vector control is executed with the same sampling frequency. The observer and the speed control loop have a sampling frequency of 5 kHz, and the speed measurement is executed with a sampling frequency of 250 Hz.

During practical implementation of the conventional MRAS scheme, it was necessary to cascade a low cutoff frequency high-pass filter with the outputs of the VM to remove integrator drift and initial condition problems. The cutoff frequency should be selected as low as possible since the purpose is just to remove the dc component, and therefore, a value of 1 Hz was chosen. Moreover, the rotor flux CM (3) and (4) did not show stable operation due to the mutual coupling between the d–q axis fluxes. Therefore, an implementation in the rotor reference frame was used instead, which eliminates the cross coupling [15], [28]. In the rotor reference frame, the rotor flux based on the CM can be written as

$$\psi_r^r = \frac{L_m}{1 + T_r s} i_s^r. \tag{10}$$

A simple dead time compensator similar to [29] and [30] is implemented, and reference voltages, which are available in the control unit, are used as the real stator voltages and will be used for both VM and NN flux observers. Hence, no stator voltage sensors are to be used.

V. Experimental Results

In this section, NN training based on experimental data will be demonstrated to overcome the problems that are mentioned in Section II. The NN is trained to match the performance of the CM, which is free from stator resistance dependence and dc-drift problems. Once the NN is trained, it is shown that it accurately matches the CM. Hence, it is possible to replace the VM with the proposed ANN. Since the performance of the conventional MRAS scheme improves at higher speeds, NN is suggested to replace the VM only in the low speed region. This will dramatically reduce the number of training samples and, consequently, the training time in addition to reducing the NN size. At high speed conventional MRAS, employing VM can be used. To further experimentally validate the proposed scheme open- and closed-loop sensorless operations will be compared for the new and conventional schemes.

A. NN Training and Testing

To generate the training data, the encodered vector control drive is run with different operating conditions in the low speed region (100 to -100 r/min), including the zero speed at various load levels ranging from 0% to 25% of the rated load. Small and large reference speed changes were applied to the drive during the training phase. The reference voltages and the measured stator currents are transformed from three phase (a, b, c) to two phase (d, q) for the NN training data. An LPF with 40 rad/s cutoff frequency was used to remove drift and noise from the reference stator voltage signals. The present and past samples of filtered stator voltages and stator current components are obtained, which will be used as inputs to the NN model. Even using direct flux sensing via search coils [18], noise and rotor slot harmonic effects on the measurements require that an LPF be used.

The outputs from the rotor flux CM, which are obtained from stator current components and encoder speed, are used as target values for the NN. This is an effective way to obtain the correct values of the rotor flux since the obtained signals are relatively noise and harmonic free, including all the drive nonlinearities. Moreover, the CM flux observer produces an accurate flux estimation even at low speed [16]. A block diagram of the training data acquisition is shown in Fig. 3.

The training is performed offline with Matlab–Simulink using the Levenberg–Marquardt training algorithm which is faster than the gradient descent back propagation algorithm but needs a large memory [18], [21]. A 5000-input/output pattern was used to train the NN. After the training, the mean squared error between targets and NN outputs decays to a satisfactory level (4.5×10^{-4}) after about 2200 epochs. The training lasts for less than 1 h on a Pentium IV PC running at 3 GHz with 512 MB of RAM.

Extensive experimental tests were carried out to test the performance of the NN observer in various operating conditions not seen during training to ensure the generalization capability of the NN model. Compared to the VM, the NN matches the CM extremely well in both transient and steady state conditions even when the drive is operating at low speed. To further validate the NN observer, three tests are conducted. The performances of both observers are compared to the CM when the encodered drive is working at 20 r/min and 5 N $\cdot$ m. Attenuation and phase delay take place in the VM due to the filter effect, whereas NN output closely tracks the CM output at this very low speed, as shown in Fig. 4(a). To test the NN observer sensitivity to parameter variation, simulations have been conducted with variations in R_s and R_r. The experimental verification of R_s sensitivity can only be done with an NN by switching an external resistor, since there is no explicit value for R_s in the observer. Although desirable, this was not attempted;

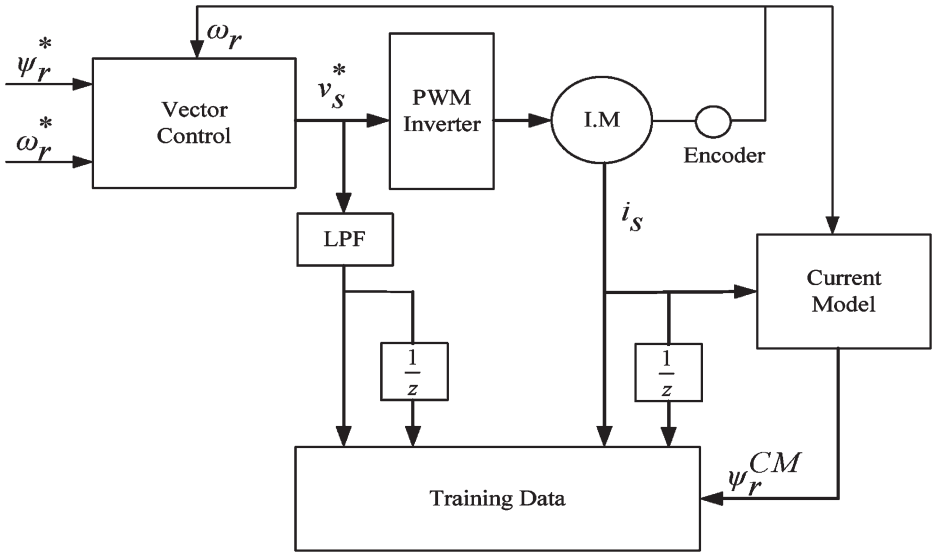

Fig. 3. NN training data acquisition.

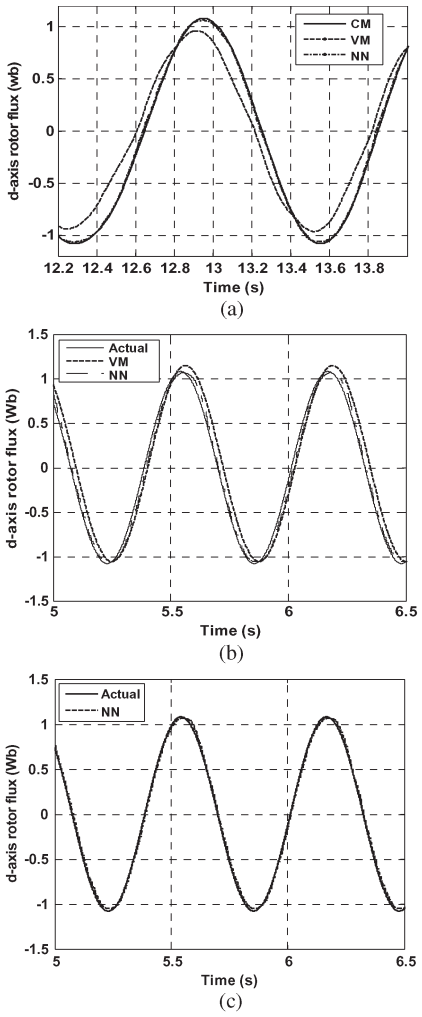

Fig. 4. NN observer testing. (a) LPF effect (experimental). (b) R_s 25% variation (simulation). (c) R_r 50% variation (simulation).

instead, simulation was used for verification. The performance of VM and NN flux observers for 25% increase in R_s is shown in Fig. 4(b). NN shows less sensitivity to R_s variation than the VM. NN observer also shows good performance with 50% R_r variation, as shown in Fig. 4(c).

These results show that the NN can fairly handle the parameter variation problem with a good level of robustness. Consequently, for integrated drive applications, where the inverter and machine are sold as one unit, the NN observer can be trained on the actual inverter–machine combination. The NN should be able to cope with the changes from these nominal parameters for other drives in the production line, which are due to the manufacturer's tolerance.

However, in a mass-production environment, where the inverter can be used with several sizes of motors, the application of this technique is more difficult. In this case, a standard NN scheme becomes unsuitable unless the training is performed during commissioning for each inverter–machine combination. This may present a drawback of the proposed method. However, this could be overcome by using a range of previously trained networks where an appropriate one can be selected according to the machine nameplate rating.

B. Open-Loop Operation

The new scheme was tested in open loop with the drive operated as an encodered vector control, i.e., the encoder speed is used for speed control and rotor flux angle estimation. The open-loop performances of the conventional and new NN-MRAS speed observers are compared. The PI controller gains of each scheme are tuned separately for optimal performance to allow a comparison between the best performances of each scheme. Figs. 5 and 6 show the open-loop performances of both schemes for a ± 30 r/min speed reversal at 10% load and disturbance rejection for a 20% step of load torque at 25 r/min. The NN-MRAS observer demonstrates better transient and steady state performance and less sensitivity to machine parameters than the conventional scheme.

An operation up to the rated load can be achieved by extending the training range of the NN observer by applying various loads ranging from 0% to 100% rated load over the same speed region, using the same training procedure described

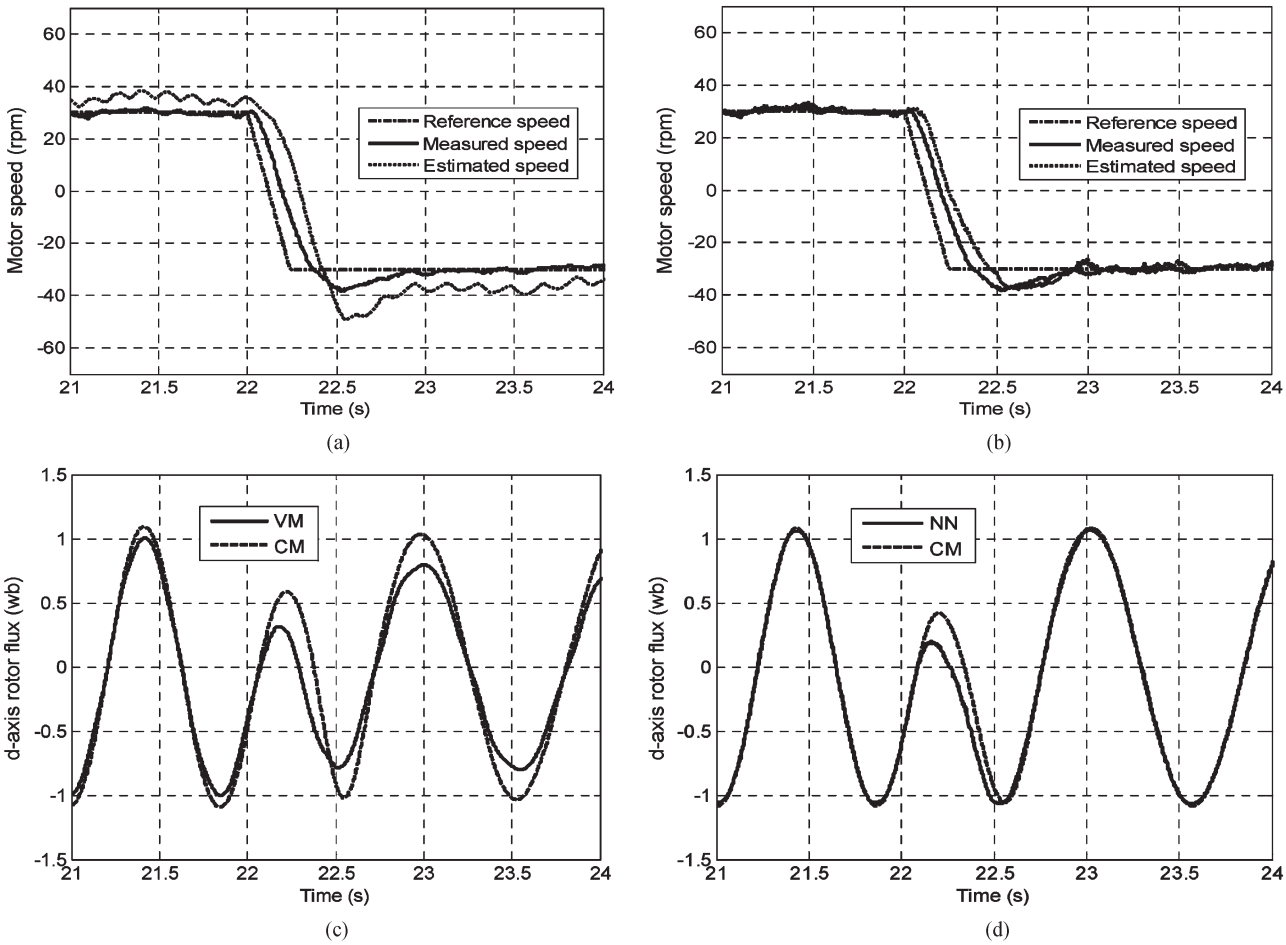

Fig. 5. Open-loop speed reversal from 30 to −30 r/min, at 10% load. Speed: (a) conventional MRAS. (b) NN MRAS. Model outputs: (c) conventional MRAS. (d) NN MRAS.

in Section V-A. The results for a ±25 r/min speed reversal at 100% rated load are shown in Fig. 7. NN-MRAS scheme performance is clearly superior to that of the classical scheme at rated load.

At low speed, a steady state error in the estimated speed is observed for the conventional MRAS observer. This is mainly due to the stator resistance mismatch between the motor and the observer. Moreover, dead time effects cannot be completely removed even by complicated compensation schemes [2]. Thus, the reference voltages used for the VM do not match the actual stator voltages across the machine terminals, representing another source for the steady state error in the estimated speed. Using the new NN-MRAS scheme completely removes the steady state error in the estimated speed and improves the load torque disturbance rejection performance of the speed observer at low speed. This improvement in the performance can be explained based on the fact that the NN estimates a flux, similar to the CM flux, which is not directly dependent on the use of the actual stator voltage, unlike the situation with the use of the VM in the conventional scheme. Moreover, no filters are needed in the flux observer with no pure integrator present in the NN model. Less sensitivity to parameter variation is given, with the new NN-MRAS scheme showing much better performance compared to the conventional MRAS observer at low and zero speeds.

C. Sensorless Closed-Loop Operation

In the following tests, the estimated speed is used for speed control and field orientation, where the drive is working as sensorless indirect rotor flux oriented. The encoder speed is used for comparison purposes only.

Tests are conducted in the low speed and at or around the zero speed region based on some recommended benchmark tests [15], [31], [32]. Selected experimental results for the tests are shown in the following section.

1) Test 1—Stair Case Speed Transients From 100 to 0 to −100 r/min at No Load: In this test, the sensorless vector control drive is subjected to a stair case speed demand from 100 r/min to zero speed in a series of five 20 r/min steps continuing to −100 r/min, at no load. The performances of both schemes are shown in Fig. 8. Stable operation is obtained for the NN-MRAS scheme, particularly around zero speed.

2) Test 2—Take Off From Zero Speed to 100 r/min After 30 s at Zero at No Load: This tests the drive capability to maintain field orientation at zero stator frequency followed by an application of a finite reference speed. The results of this benchmark test are shown in Fig. 9. Unstable operation at zero speed was observed for the conventional MRAS with oscillation around zero speed. The NN MRAS proves its ability to hold the zero speed at no load without any oscillations. Both schemes succeed in taking off to 100 r/min after 30 s at zero speed.

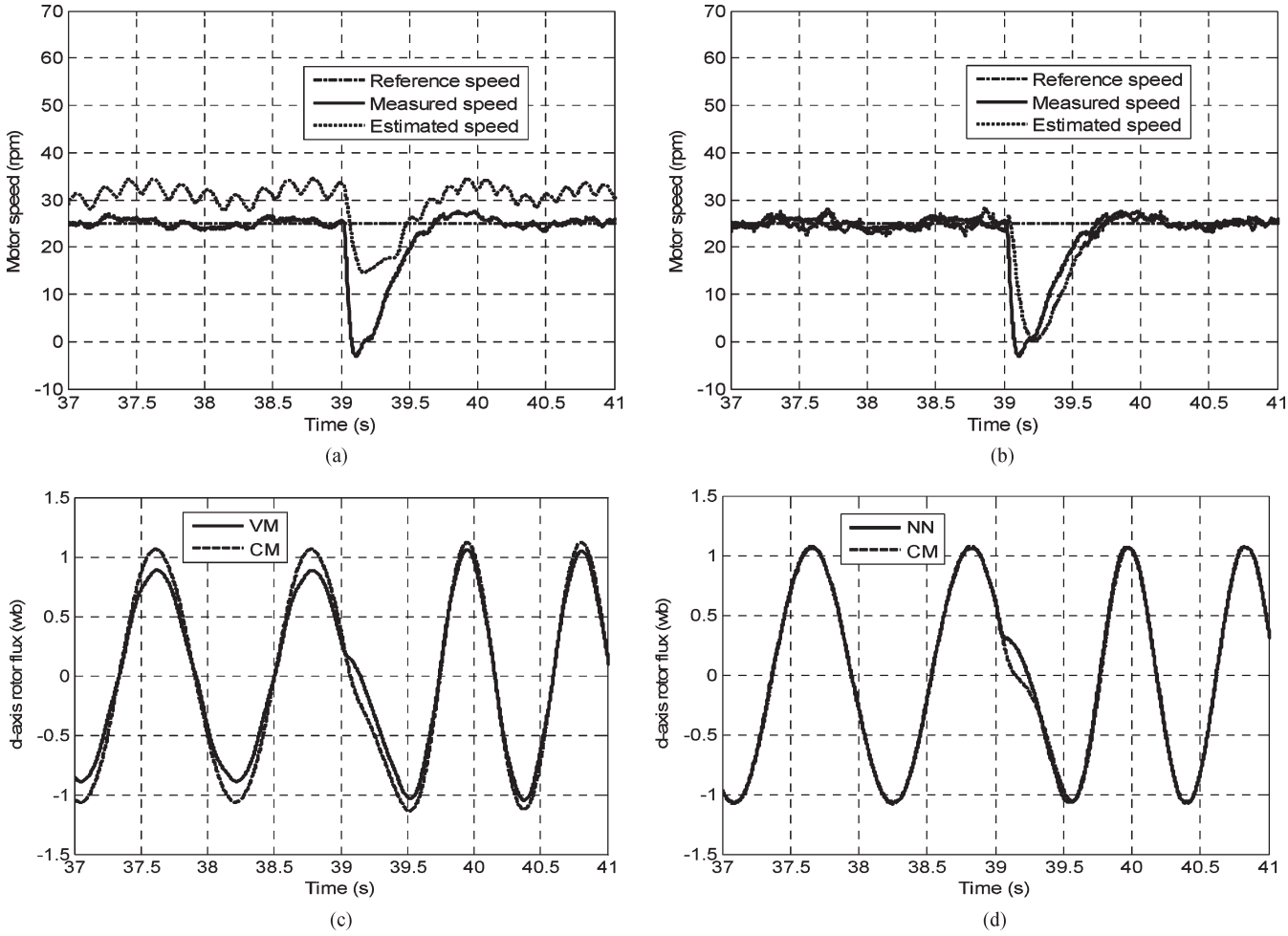

Fig. 6. Open-loop 20% load torque disturbance rejection, 25 r/min. Estimated speed: (a) conventional MRAS. (b) NN MRAS. Model outputs: (c) conventional MRAS. (d) NN MRAS.

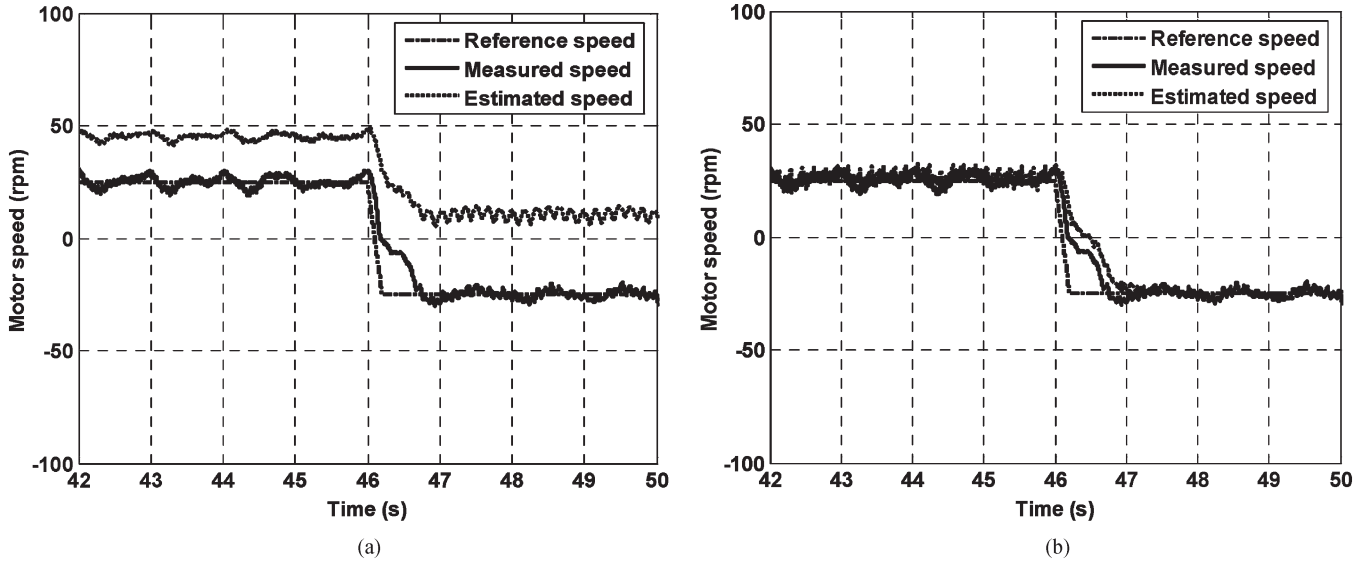

Fig. 7. Open-loop speed reversal from 25 to −25 r/min, at a rated load (100% load torque). Speed: (a) conventional MRAS. (b) NN MRAS.

3) Test 3—Speed Step Down From 20 to 0 r/min in Three Steps Each of 10 r/min at 10% Load: This tests the performance of the sensorless drive at very low and zero speeds with load. The results are shown in Fig. 10. At a reference speed of 20 r/min, the NN-MRAS scheme was stable, showing less steady state error compared to the conventional one. At such speeds and below, the conventional MRAS fails to provide stable operation, giving large oscillations.

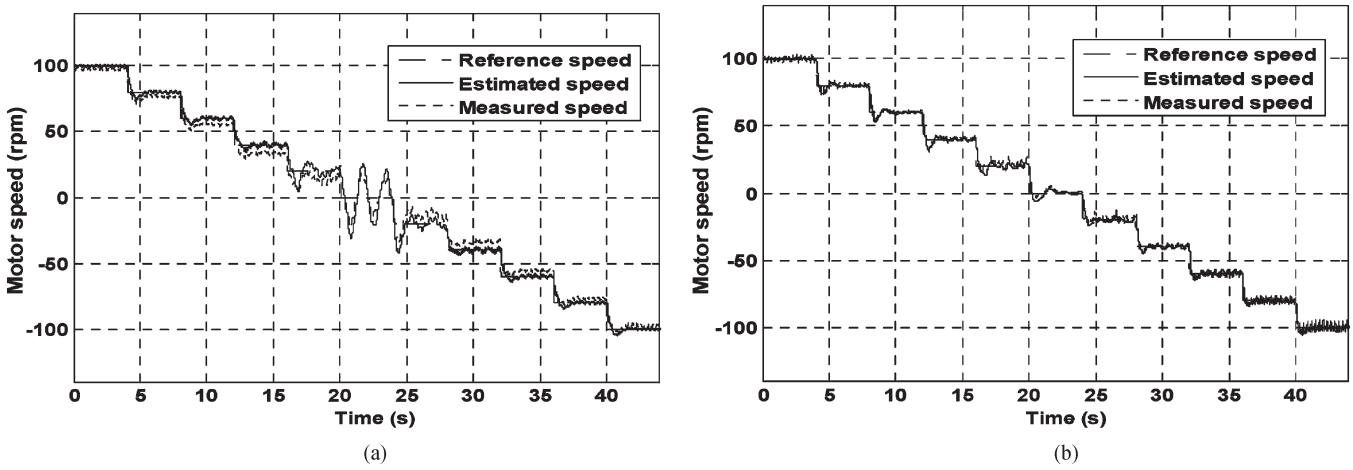

Fig. 8. Sensorless performance for benchmark test 1, at no load. Speed: (a) conventional MRAS. (b) NN MRAS.

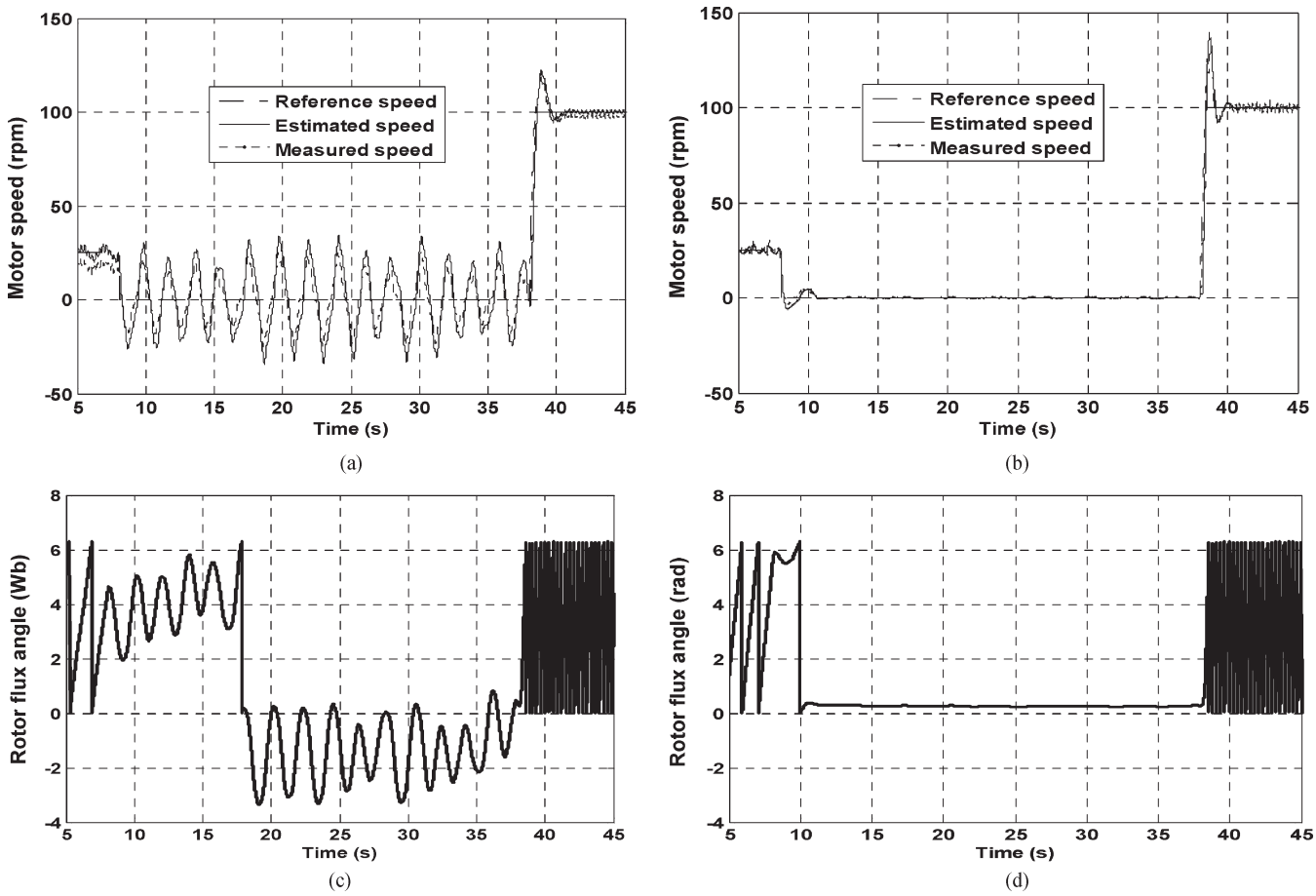

Fig. 9. Sensorless result of benchmark test 2, at no load. Speed: (a) conventional MRAS. (b) NN MRAS. Rotor flux position: (c) conventional MRAS. (d) NN MRAS.

4) Test 4—20% Load Torque Rejection at 50 r/min: This test examines the load torque disturbance rejection capability of the sensorless drive. Both schemes have been tested when a 20% step change in load torque is applied at 50 r/min. The NN MRAS shows better dynamic and steady state performance with negligible steady state error between the actual and estimated speeds, as shown in Fig. 11.

5) Test 5—±25 r/min Speed Reversal at 10% Load: This last test shows the drive performance for a very low speed reversal under load torque. A ±25 r/min speed reversal demand was applied to the drive when working at 10% load. Better performance with negligible steady state error was obtained from NN-MRAS observer compared to the conventional MRAS scheme, as shown in Fig. 12. A summary of test results from zero to full

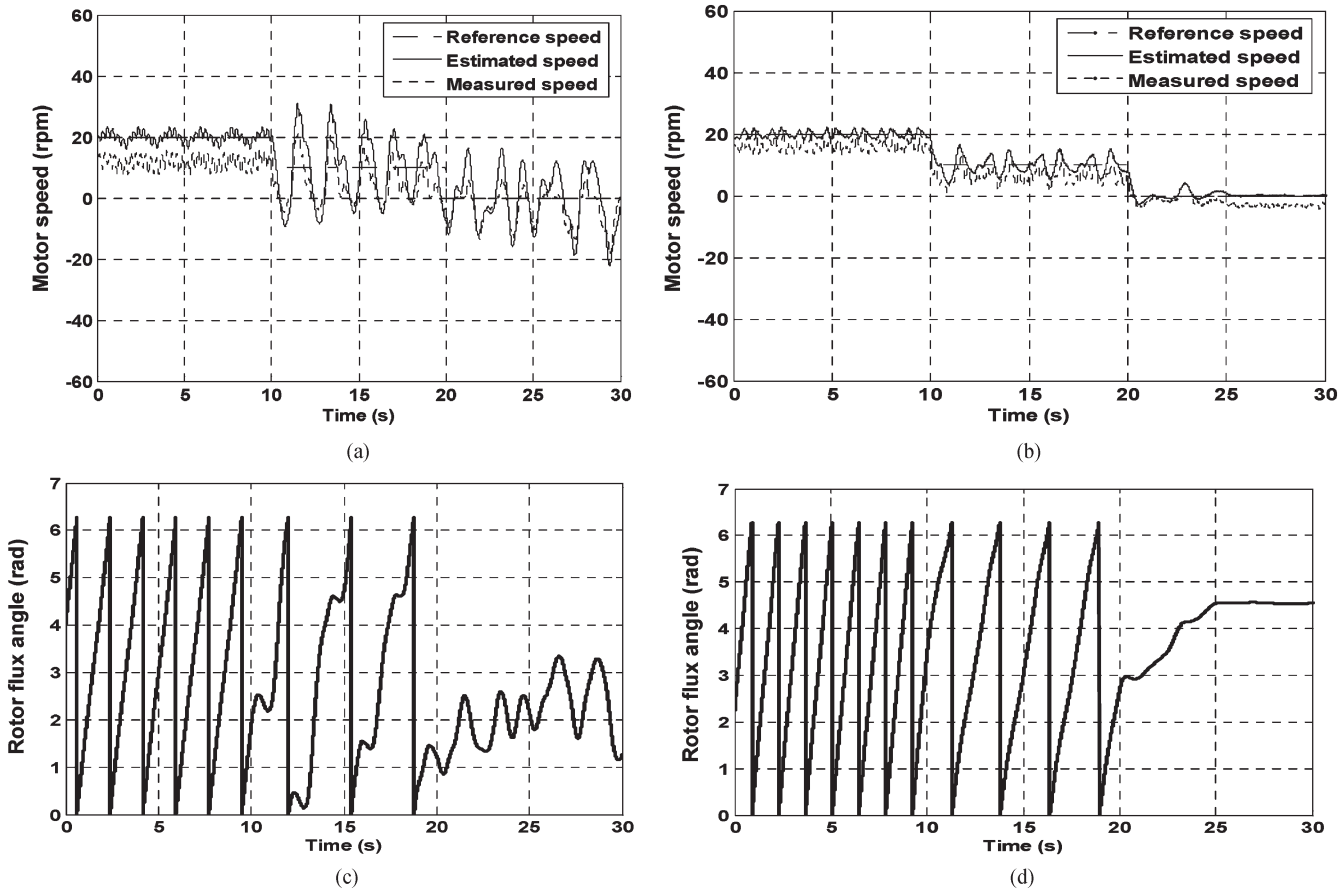

Fig. 10. Sensorless result of benchmark test 3, at 10% load. Speed: (a) conventional MRAS. (b) NN MRAS. Rotor flux position: (a) conventional MRAS. (b) NN MRAS.

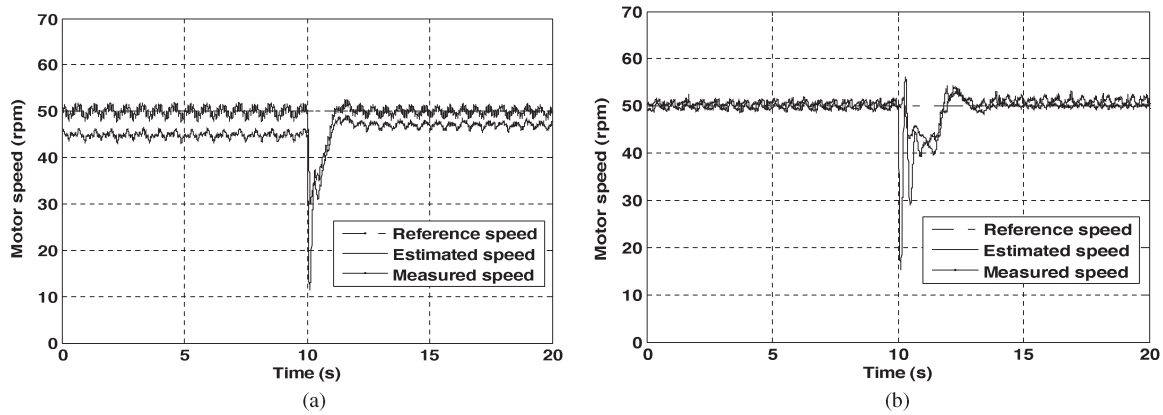

Fig. 11. Sensorless performance for benchmark test 4, at 20% load torque rejection, at 50 r/min. Speed: (a) conventional MRAS. (b) NN MRAS.

load using the conventional and new schemes is given in Table I, showing the superior behavior of the new scheme under various load conditions.

VI. Conclusion

This paper has presented an entirely new application of an NN to give an improved MRAS speed observer scheme suitable for speed sensorless induction motor drives. A multilayer feedforward NN estimates the rotor flux components from present and past samples of reference stator voltages and measured currents. The new scheme makes use of the offline-trained NN observer as a reference model in MRAS scheme. Training data are obtained from experiments without the need for search coils. Using the new NN scheme for flux estimation eliminates the need for pure integration with less sensitivity to stator resistance variations.

The results obtained from a systematic set of benchmark experimental tests using a 7.5-kW induction motor drive system prove the great improvement of the sensorless drive performance around and at zero speed. Open-loop tests show that the steady state error in the estimated speed has been

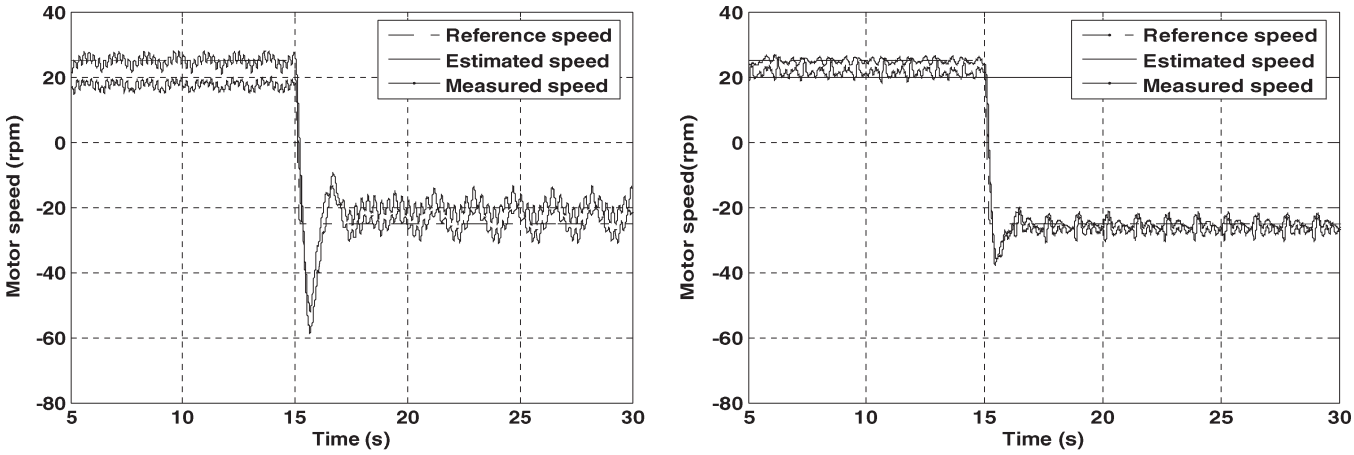

Fig. 12. Sensorless performance for benchmark test 5, at ±25 r/min speed reversal, at 10% load. Speed: (a) conventional MRAS. (b) NN MRAS.

TABLE I
SUMMARY OF TEST RESULTS

	25 rpm 100% rated load Open loop	-25 rpm 100% rated load Open loop	Zero speed No load Sensorless	Zero speed 10% load Sensorless	Zero speed 20% load Sensorless	20 rpm 10% load Sensorless	10 rpm 10% load Sensorless	50 rpm 20% load Sensorless	-25 rpm 10% load Sensorless	-25 rpm 25% load Sensorless
Conv. MRAS	20 rpm steady state error	35 rpm steady state error	Unstable	Unstable	Unstable	10 rpm steady state error	Unstable	3 rpm steady state error	5 rpm steady state error	Unstable
NN MRAS	Negligible steady state error	Negligible steady state error	Zero steady state error	3 rpm steady state error	7 rpm steady state error	4 rpm steady state error	3 rpm steady state error	1 rpm steady state error	Negligible steady state error	7 rpm steady state error

totally removed compared to the conventional observer using a VM. Closed-loop sensorless operation is greatly improved at very low and zero speeds without using voltage sensors.

APPENDIX
MOTOR PARAMETERS

Three-phase 7.5-kW 415-V delta-connected 50-Hz four-pole Star equivalent parameters are as follows: $R_s = 0.7767\ \Omega$, $R_r = 0.703\ \Omega$, $L_s = 0.10773$ H, $L_r = 0.10773$ H, $L_m = 0.10322$ H, and $J = 0.22\ \text{kg} \cdot \text{m}^2$.

REFERENCES

[1] J. W. Finch and D. Giaouris, "Controlled AC electrical drives," *IEEE Trans. Ind. Electron.*, vol. 55, no. 2, pp. 481–491, Feb. 2008.

[2] J. Holtz and J. Quan, "Drift and parameter compensated flux estimator for persistent zero stator frequency operation of sensorless controlled induction motors," *IEEE Trans. Ind. Appl.*, vol. 39, no. 4, pp. 1052–1060, Jul./Aug. 2003.

[3] M. Rashed and A. F. Stronach, "A stable back-EMF MRAS-based sensorless low speed induction motor drive insensitive to stator resistance variation," *Proc. Inst. Elect. Eng.—Electr. Power Appl.*, vol. 151, no. 6, pp. 685–693, Nov. 2004.

[4] V. Vasic and S. Vukosavic, "Robust MRAS-based algorithm for stator resistance and rotor speed identification," *IEEE Power Eng. Rev.*, vol. 21, no. 11, pp. 39–41, Nov. 2001.

[5] F. Peng and T. Fukao, "Robust speed identification for speed-sensorless vector control of induction motors," *IEEE Trans. Ind. Appl.*, vol. 30, no. 5, pp. 1234–1240, Sep./Oct. 1994.

[6] C. Schauder, "Adaptive speed identification for vector control of induction motors without rotational transducers," *IEEE Trans. Ind. Appl.*, vol. 28, no. 5, pp. 1054–1061, Sep./Oct. 1992.

[7] P. Vas, *Sensorless Vector and Direct Torque Control*. New York: Oxford Univ. Press, 1998.

[8] S. Maiti, C. Chakraborty, Y. Hori, and M. C. Ta, "Model reference adaptive controller-based rotor resistance and speed estimation techniques for vector controlled induction motor drive utilizing reactive power," *IEEE Trans. Ind. Electron.*, vol. 55, no. 2, pp. 594–601, Feb. 2008.

[9] M. S. Zaky, M. M. Khater, S. S. Shokralla, and H. A. Yasin, "Wide-speed-range estimation with online parameter identification schemes of sensorless induction motor drives," *IEEE Trans. Ind. Electron.*, vol. 56, no. 5, pp. 1699–1707, May 2009.

[10] Y. A. Kwon and D. W. Jin, "A novel MRAS based speed sensorless control of induction motor," in *Proc. 25th Annu. Conf. IEEE Ind. Electron. Soc.*, 1999, pp. 933–938.

[11] L. Ben-Brahim, S. Tadakuma, and A. Akdag, "Speed control of induction motor without rotational transducers," *IEEE Trans. Ind. Appl.*, vol. 35, no. 4, pp. 844–850, Jul./Aug. 1999.

[12] B. Karanayil, M. F. Rahman, and C. Grantham, "An implementation of a programmable cascaded low-pass filter for a rotor flux synthesizer for an induction motor drive," *IEEE Trans. Power Electron.*, vol. 19, no. 2, pp. 257–263, Mar. 2004.

[13] M. Comanescu and L. Xu, "Sliding mode MRAS speed estimators for sensorless vector control of induction machine," *IEEE Trans. Ind. Electron.*, vol. 53, no. 1, pp. 146–153, Feb. 2006.

[14] M. Hinkkanen and J. Luomi, "Modified integrator for voltage model flux estimation of induction motors," *IEEE Trans. Ind. Electron.*, vol. 50, no. 4, pp. 818–820, Aug. 2003.

[15] Q. Gao, C. S. Staines, G. M. Asher, and M. Sumner, "Sensorless speed operation of cage induction motor using zero drift feedback integration with MRAS observer," in *Proc. Eur. Conf. Power Electron. Appl.*, 2005, pp. P.1–P.9. [Online]. Available: http://ieeexplore.ieee.org/xpl/freeabs_all.jsp?arnumber=1665428

[16] C. C. Lascu, I. Boldea, and F. Blaabjerg, "A modified direct torque control for induction motor sensorless drive," *IEEE Trans. Ind. Appl.*, vol. 36, no. 1, pp. 122–130, Jan./Feb. 2000.

[17] L. M. Grzesiak and B. Ufnalski, "Neural stator flux estimator with dynamical signal preprocessing," in *Proc. IEEE AFRICON*, 2004, pp. 1137–1142.

[18] A. Ba-Razzouk, A. Cheriti, G. Olivier, and P. Sicard, "Field oriented control of induction motors using neural network decouplers," *IEEE Trans. Power Electron.*, vol. 12, no. 4, pp. 752–763, Jul. 1997.

[19] Y. Yusof and A. H. Yatim, "Simulation and modelling of stator flux estimator for induction motor using artificial neural network technique," in *Proc. Nat. Power Energy Conf.*, 2003, pp. 11–15.

[20] P. Vas, *Artificial-Intelligence-Based Electrical Machines and Drives-Application of Fuzzy, Neural, Fuzzy-Neural and Genetic Algorithm Based Techniques*. New York: Oxford Univ. Press, 1999.
[21] B. K. Bose, "Neural network applications in power electronics and motor drives—An introduction and perspective," *IEEE Trans. Ind. Electron.*, vol. 54, no. 1, pp. 14–33, Feb. 2007.
[22] J. Campbell and M. Sumner, "Practical sensorless induction motor drive employing an artificial neural network for online parameter adaptation," *Proc. Inst. Elect. Eng.—Electr. Power Appl.*, vol. 149, no. 4, pp. 255–260, Jul. 2002.
[23] B. Karanayil, M. F. Rahman, and C. Grantham, "Online stator and rotor resistance estimation scheme using artificial neural networks for vector controlled speed sensorless induction motor drives," *IEEE Trans. Ind. Electron.*, vol. 54, no. 1, pp. 167–176, Feb. 2007.
[24] M. Cirrincione and M. Pucci, "An MRAS-based sensorless high-performance induction motor drive with a predictive adaptive model," *IEEE Trans. Ind. Electron.*, vol. 52, no. 2, pp. 532–551, Apr. 2005.
[25] M. Cirrincione, M. Pucci, G. Cirrincione, and G. A. Capolino, "Sensorless control of induction machines by a new neural algorithm: The TLS EXIN neuron," *IEEE Trans. Ind. Electron.*, vol. 54, no. 1, pp. 127–149, Feb. 2007.
[26] M. Cirrincione, M. Pucci, G. Cirrincione, and G. Capolino, "A new adaptive integration methodology for estimating flux in induction machine drives," *IEEE Trans. Power Electron.*, vol. 19, no. 1, pp. 25–34, Jan. 2004.
[27] M. Gallegos, R. Alvarez, C. Nunez, and V. Cardenas, "Effects of bad currents and voltages acquisition on speed estimation for sensorless drives," in *Proc. Electron., Robot. Automotive Mech. Conf.*, 2006, pp. 215–219.
[28] P. L. Jansen and R. D. Lorenz, "A physically insightful approach to the design and accuracy assessment of flux observers for field oriented induction machine drives," *IEEE Trans. Ind. Appl.*, vol. 30, no. 1, pp. 101–110, Jan./Feb. 1994.
[29] S. H. Kim, T. S. Park, J. Y. Yoo, G. T. Park, and N. J. Kim, "Dead time compensation in a vector-controlled induction machine," in *Proc. Power Electron. Spec. Conf.*, 1998, pp. 1011–1016.
[30] L. Ben-Brahim, "On the compensation of dead time and zero-current crossing for a PWM-inverter-controlled AC servo drive," *IEEE Trans. Ind. Electron.*, vol. 51, no. 5, pp. 1113–1117, Oct. 2004.
[31] K. Ohyama, G. M. Asher, and M. Sumner, "Comparative experimental assessment for high-performance sensorless induction motor drives," in *Proc. IEEE Int. Symp. Ind. Electron.*, 1999, vol. 1, pp. 386–391.
[32] K. Ohyama, G. M. Asher, and M. Sumner, "Comparative analysis of experimental performance and stability of sensorless induction motor drives," *IEEE Trans. Ind. Electron.*, vol. 53, no. 1, pp. 178–186, Feb. 2006.

Shady M. Gadoue (M'06) was born in Cairo, Egypt, in 1978. He received the B.Sc. (with honors) and M.Sc. degrees in electrical engineering from the Faculty of Engineering, Alexandria University, Alexandria, Egypt, in 2000 and 2003, respectively, and the Ph.D. degree in the area of sensorless control of induction motor drives from Newcastle University, Newcastle upon Tyne, U.K., in 2009.

He is with the Department of Electrical Engineering, Alexandria University, where he worked as a Demonstrator in 2000 and an Assistant Lecturer in 2003 and is currently a Lecturer on electrical machines and drives. His main research interests are in the area of estimation and control in electric drives and power electronics. His current research activities relate to sensorless control of induction motor drives using artificial intelligence techniques.

Damian Giaouris (M'01) was born in Munich, Germany, in 1976. He received the Diploma in automation engineering from the Automation Department, Technological Educational Institute of Thessaloniki, Thessaloniki, Greece, in 2000, and the M.Sc. degree in automation and control with distinction and the Ph.D. degree in the area of control and stability of induction machine drives from Newcastle University, Newcastle upon Tyne, U.K., in 2001 and 2004, respectively.

He is currently a Lecturer on control systems with the School of Electrical, Electronic and Computer Engineering, Newcastle University. His research interests are advanced nonlinear control, estimation, and digital signal processing methods applied to electric drives and electromagnetic devices, and nonlinear phenomena in power electronic converters.

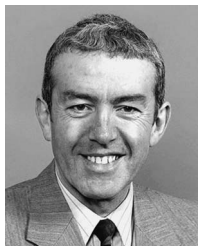

John W. Finch (M'90–SM'92) was born in Durham, U.K. He received the B.Sc.(Eng.) degree (with first class honors) in electrical engineering from University College London (UCL), London, U.K., and the Ph.D. degree from the University of Leeds, Leeds, U.K.

He was a Consultant to many firms and was an Associate Director with the Resource Centre for Innovation and Design, helping companies with developments. He is currently an Emeritus Professor of electrical control engineering with the School of Electrical, Electronic and Computer Engineering, Newcastle University, Newcastle upon Tyne, U.K. He has authored or coauthored 150 publications on applied control and simulation of electrical machines and drives.

Prof. Finch was a winner of the Goldsmid Medal and Prize (UCL Faculty prize), the Carter Prize (Leeds University postgraduate prize), and the IET's Heaviside, Kelvin, and Hopkinson Premiums. He is an IET Fellow and is also a Chartered Engineer in the U.K.